A Gill-type mechanism for rainfall initiation over the rainshadow region

T. S. Mohan[1], Kondapalli Niranjan Kumar[1], A. Madhulatha[3] , M. Rajeevan[2]

1. National Centre for Medium Range Weather Forecasts, Ministry of Earth Sciences, India
2. Ministry of Earth Sciences, New Delhi, India
3. Korean Institute of Atmospheric Prediction System, Seoul, South Korea

Key words:

Wet spells, Southeast India, Rainshadow region, Monsoon, Rossby waves, Maritime continent

Corresponding author:

Mohana S. Thota
Scientist, National Center for Medium Range Weather Forecasting,
Ministry of Earth Sciences, Noida-62, 201309, U.P. India.
drmohanthota@gmail.com; mohant@ncmrwf.gov.in

Abstract

This novel study explains a physical mechanism for the rainfall initiation over the southeast peninsular India (SEPI, referred to be a 'rain shadow' region) during the southwest monsoon season. Further, the contrasting rainfall patterns between the rain shadow region and central India (CI,) are also elucidated through the response of the maritime continent (MRC) convection. The MRC is found to be a prominent source for the initiation of wet spells over the rain shadow region (during which CI is in dry phase), with the rainfall anomalies over MRC leads SEPI by ~5-7 days. Evolution of convective anomalies resembles a classical Gill-type response, with a pair of Rossby waves on the poleward side of the convection center and Kelvin waves on the eastern side. Thus, the combined effect of large-scale circulation and moisture anomalies over MRC contributes to the preconditioning and subsequent positive rainfall anomalies over the rain shadow region.

1. Introduction:

During boreal summer monsoon season, pronounced intraseasonal oscillations (ISO) over Indian subcontinent are characterized by poleward propagation of convective anomalies from equatorial regions (Yasunari 1976; Sikka and Gadgil 1980), resulting in alternative transition of active (enhanced rainfall) and break (subdued rainfall) spells (Krishnamurti and Bhalme 1976; Lawerence and Webster, 2002; Gadgil 2003; Goswami 2005; Rajeevan et al 2006, 2010). The circulation anomalies associated with these active/break spells cover up the entire Indian subcontinent and adjacent oceanic regions (Webster et al. 1998; Gadgil 2003; Goswami 2005). During these periods, the ISO phase is not coherent over the Indian subcontinent but exhibits large spatial variations (Webster et al. 1998; Annamalai and Slingo 2001; Gadgil 2003; Goswami 2005; Rajeevan et al. 2006; Rao et al. 2009; Rajeevan et al. 2010). This results in a large spatial variability in rainfall intensities between central India (CI; monsoon zone, 21-27N, 72-85E) and southeast peninsular India (SEPI, 9-15N, 77-81E) (Rao et al. 2009; Mohan et. al. 2018). In general, widespread rainfall activity primarily occurs over the west coast of India due to orography and over the CI region during the active phase of the summer monsoon (Sikka and Gadgil 1980; Goswami et al. (2003); Rajeevan et al. 2010; Rao et al. 2009; Mohan et al 2018). In contrast, rainfall over the SEPI region largely occurs due to the isolated thunderstorms with a secondary contribution from sea-breeze circulations near the southeast coast (Simpson et al. 2007). Further, SEPI is an agrarian region that contains important cities crucial for trade and economic growth of the country, rice bowls, spaceport, etc. Besides, SEPI is considered to be the rain shadow region during the summer monsoon season, since it is situated on the lee-ward side of the west coast (Monsoon monograph, 2012).

In the recent past, considerable effort has been given to understand the sources of these monsoon ISO's their variability and predictability from both the models and observations,

over Indian region (Gadgil 2003; Goswami 2005; Rajeevan et al. 2006, 2010; Prasanna and Annamalai 2012; Mohan et al. 2018 and references therein). Despite its importance and uniqueness, very few studies exist on rainfall variability over SEPI at intraseasonal time scales. For instance, recent studies have explored the dynamical and thermodynamical aspects of the SEPI region during south-west monsoon and found significant differences with the CI (Rao et al. 2009; Mohan and Rao 2012; Mohan and Rao 2017; Mohan et al. 2018a). However, the physical mechanism responsible for the initiation of these monsoon spells, in particular wet spells, are not studied and needs considerable attention. This forms our primary objective of the present study. Note, here the terminology "wet spell" is used over SEPI instead of "active" to avoid confusion from the active monsoon phase over CI. Thus, the current study is based on the following objectives

i) What are the factors influencing the contrasting spells over the rain shadow region and the core monsoon zone?

ii) What is the physical mechanism responsible for the initiation of positive rainfall anomalies over the rain shadow region during wet spells?

In this study, we try to address these questions by investigating the role of large-scale circulations emphasizing equatorial wave dynamics and establish a link in the initiation of wet spells (positive rainfall anomalies) over the SEPI region.

2. Method and Data used:

We have used a suite of precipitation data from India Meteorological Department (IMD) and Tropical Rainfall Measuring Mission (TRMM) 3B42 daily product having a spatial resolution 0.25°, for studying the evolution of rainfall anomalies. Due to the non-availability of long period TRMM precipitation data, only 18 monsoon seasons (1998-2015) for the construction of space-time evolution of rainfall anomalies. Daily rainfall anomalies are computed from the

data by removing the climatological rainfall mean from the respective calendar day and these anomalies are used for composite analysis. Further, the significance of the composites is computed using the student's test. Three-dimensional data of temperature (T), specific humidity (q), vertical velocity (ω), cloud liquid water (CLW) and horizontal wind component data (u,v), at daily intervals obtained from European Center for Medium Range Weather Forecast (ECMWF) Reanalysis (ERA 5; ECMWF 2017; Hersbach and Dee 2016), are used to investigate the vertical and space-time evolution. The spatial resolution of the data is 0.25° (approximately 28 km), with 27 pressure levels between 100 and 1000 hPa.

The identification of wet and dry monsoon spells over SEPI is carried out using the methodology by Mohan and Rao (2012) over SEPI using high-resolution (0.25° × 0.25°) IMD gridded daily rainfall data for the period 1980–2015. First, the time series of daily average rainfall for each year as well as climatological time series (from 36 years of data) are prepared. If the rainfall on at least 3 consecutive days is more than the rainfall threshold (climatological rainfall + standard deviation) for those days, then the period is considered as a wet spell.

3. Results

Mean seasonal (June through September) summer monsoon rainfall is not homogeneous (Figure 1a1), rather exhibits spatial variations (Figure 1a1) over the Indian region. High rainfall amounts (>14 mm/day) are observed over the West coast and North-eastern India due to complex orography over these regions. Climatological rainfall amounts over SEPI was considerably less (< 4mm/day) compared to CI (8-12 mm/day). The spatial variation of rainfall over India mainly depends on duration and occurrence time of active/break spells (Goswami and Ajayamohan 2001; Goswami et al. 2003). Therefore, we show the rain fraction, which will provide better insight into rainfall characteristics in wet/dry spells.

Rainfall fraction is the ratio between rainfall during wet/dry days to the total rainfall during the monsoon period (Rao et al., 2009). SEPI region receives < 10% of the seasonal rainfall during dry spells while central and northern parts of India receive > 40% due to the persistent active monsoon conditions (Figure 1a2). In contrast, the SEPI region receives ~40-50% of rainfall during break conditions over CI (Figure 1a3) which is noteworthy. Thus, it is important to note that the SEPI region receives a significant amount of rainfall during all India break conditions as shown in Figure 1a3. Further, the spatial patterns of rainfall fraction indicate the prominent out of phase relation between SEPI and CI corroborating with the earlier studies Motivated by the reversal in the spatial patterns in rainfall fractions during dry/wet spells and the rainfall contribution between SEPI and CI, the question of interest here is what factors govern the rainfall over SEPI when the core monsoon zone is experiencing break conditions?.A composite analysis is performed in the following sections to explore the contrasting features between CI and SEPI regions.

3.1 Space-time evolution

We showed the composite space-time evolution of rainfall anomalies from -10 to +6 days with 2-day intervals were shown in Figure 1b. During lag -10 to -8 days, positive rainfall anomalies > ~3 mm covered over eastern equatorial Indian ocean and maritime continent (MRC, 10S-5N, 90-110E). During this period, positive rainfall anomalies are absent over SEPI and most of the Indian subcontinent (Figure 1b1 and 1b2). From lag -6 and -4 days, onwards positive rainfall anomalies (~ 1-2 mm/day) start to appear over the SEPI region. During this period large negative rainfall anomalies (>- 6mm/day) are seen over most of the Bay of Bengal (BoB) region, which extends up to south china sea (SCS) resembling the tilting rainfall band structure (Annamalai and Slingo 2001) (Figure 1b3 and 1b4). With time, at lag “0” (i.e. during peak wet spell day) the enhanced positive rainfall anomalies (~6 mm/day) occupied over the entire SEPI region. A dipole rainfall anomaly pattern is seen

between CI and SEPI (Figure 1b6) during lag 0 days reconfirms that CI and SEPI regions indeed exhibit out of phase relationship during monsoon. The rainfall anomalies exhibit two elongated tilted structures, one from the MRC to SEPI, with another branch having similar magnitudes, extended to the south of the Equator (Figure 1b5 and 1b6). Movement of the northern branch of the rainfall band is relatively quick and now seen around the parts of the Arabian sea and west coast. In the subsequent lags, from +2 to +4 days, the magnitude of positive rainfall anomalies is further reduced (Figure 1b7 and 1b8) over SEPI. Thereafter rainfall anomalies over SEPI (central India) exhibit negative (positive) indicating another cycle of monsoon convection. Time evolution of area averaged rainfall anomalies over SEPI and MRC show the leading nature of the MRC rainfall anomalies by ~5-7 days (Figure S1) indicating the mutual interaction of these two regions during the boreal summer monsoon. Whilst, Figure 1, shows the composite rainfall evolution of the convective environment over SEPI, it is important to know the level at which the moistening peaks and associated vertical stability for the initiation of these wet spells.

3.2 Vertical structure:

Figure 2 (a-h) shows the evolution of composite vertical profiles of static stability (combined T and q), anomalous vertical velocity (ω'), and cloud liquid water (CLW), during wet spells over SEPI (Figure 2a-d) and MRC (Figure 2e-h).

Over SEPI, at lags between day 0 to +5 day, a tripole structure is seen in T' profile with cooling (<-0.5 K) in the lower (below ~ 850 hPa) and upper troposphere (100-250 hPa) due to evaporation and radiative processes respectively, and moderate warming T'(~0.2) between 250-850 hPa (Figure 2a). However, over MRC despite the presence of cooling in the boundary layer heights during -5 to +5 days, a clear tripole structure in T is not seen (Figure 2e). Presence of cooling (warming) in the lower (middle) troposphere is also observed during

155 the wet spell of the Australian (Williams et al., 1992; McBride and Frank, 1999) and Indian
156 (Bhat et al., 2002; Webster et al., 2002) monsoon systems, especially over the oceans. The
157 present analysis does not show significant warming in the middle troposphere during the wet
158 spell, except for those two height regions (500-700 hPa and 250-400 hPa) (Figure 2a). The
159 longwave cooling seen in the middle troposphere is gradually intensified (>-0.5 K) with time
160 till lag +15 day. Further, between +5 to +15 days presence of cooling (~ -0.3 K) around 700
161 hPa, perhaps induce the stable layers and affect the convective growth as evidenced by the
162 negative rainfall tendencies (Figure S1a).

163 Moisture anomalies (q') distributed vertically from surface to 400 hPa during the lags -5 to
164 +5 days over SEPI (Figure 2b). Pre-moistening of the atmosphere from -10 days onwards is
165 seen around boundary layer heights below 700 hPa level and with time the positive q
166 anomalies enhanced and reached upto 400hPa level with peak (> 0.5 g/kg) around 650-700
167 hPa. Interestingly, the moistening over the MRC region is leading SEPI by ~7 days and the
168 vertical distribution of the q' is also limited compared to that of SEPI (Figure 2f). Time
169 evolution of the boundary layer averaged moisture anomalies over SEPI and MRC reaffirms
170 that the lead time is not only in the rainfall but also seen in the boundary layer moisture
171 (Figure S2b). It is known from the earlier studies that the low-level moisture increases before
172 the peak precipitation promotes the development of deep convection (Kikuchi and Takayabu
173 2004, Benedict and Randall 2009, Lau and Waliser 2012).

174 The maximum upward motion (ω'>-0.04 Pa/s) is confined between -5 to +5 days over SEPI,
175 with peak magnitudes around 250-300 hPa level. On the other hand, peak vertical motion
176 around 400hPa over the MRC region indicates that the diabatic heating and corresponding
177 cloud vertical structures are relatively shallow. The presence of relatively low-level ascent
178 over MRC compared to SEPI is also substantiate by the vertical profile of CLW (Figure 2h).
179 Moderate descent (~0.002 Pa/s) around -15 days in boundary layer heights below 700 hPa

and weak ascent (-0.003 Pa/s) until -10 days combined with lack of sufficient moisture ($q'<$ 0.2 g/kg) seizures convective growth before the initiation of a wet spell (Figure S1a and Figure 2b). Similar descent and dryness also have seen +15 days, as a result, negative tendencies in the rainfall anomalies are seen over SEPI. Lead-lag composites of CLW (Figure 2d and 2h) show completely different vertical structures over SEPI and MRC respectively. For instance, over SEPI low-level positive CLW values (<0.2 g/m3) shows the presence of shallow clouds. With time these CLW shows enhancement and distributes vertically and reaches a maximum at ~300-400 hPa level. In contrast over MRC, the vertical structure of CLW exhibits bi-modal distribution with one peak around the boundary layer heights and the second peak around 450-500 hPa level. It is noted that the magnitude of the second peak is relatively large due to the presence of water coated ice at 0° C isotherm level (Kollias et al. 2009). The magnitude of CLW during the wet spells over SEPI and the transformation of shallow to deep convection over tropical regions are corroborating with earlier studies over tropical regions by Kikuchi and Takayabu 2004; Madhulatha et al. (2020).

3.3. Boundary layer linkage:

As mentioned in section 3.2, the build-up of low-level moisture anomalies and associated heating over MRC (Figure 2f and 2g) enhances the boundary layer convergence and induces the low-level equatorial Kelvin wave (Hendon and Sallby 1994, Kiladis and Straub 2005). This low-level convergence increases low-level moist static energy (MSE) (Figure S1c) and destabilization occurs (Wang 2018; Hsu and Li 2012). The present analysis shows that the destabilization occurs ~7-10 days earlier in the MRC region in the boundary layer (Figure S1c). The low-level moisture and MSE anomalies discussed above clearly indicate the leading nature in the initiation of the precipitation anomalies over the SEPI region. To further strengthen our argument, we show the composite latitude-time structure of boundary layer averaged *q*-anomalies over MRC longitudes (110-120 E) (Fig. S1d). A well-marked

205 northward propagating positive *q* anomalies from the equatorial regions are seen from lag -
206 10day onwards and by lag "0" the anomalies reached ~13 N and with time they further
207 propagated north, but with less intensity (Figure S1d).

208 *3.4 Moisture Source:*

209 Analysis of vertical profiles of *q*' (Figure 2) indicates boundary layer moistening before the
210 peak rainfall over SEPI. Thus, identifying the source of this preconditioning is necessary,
211 which plays a crucial role in inducing the convective environment favorable for the initiation
212 of wet spells.

213 *(a) Role of Equatorial waves*

214 In general, convective anomalies initiate over the Western Indian Ocean (WIO) and move
215 eastward and upon reaching MRC the anomalies reduce its intensity and decay (Hung and Sui
216 2018). Figure 3 shows the space-time evolution of the composite maps of OLR, winds at 850
217 and 200 hPa level and vertical velocity relative to the peak wet spell (lag 0) over SEPI. Note
218 that for better legibility, the evolution of these parameters was given from lag -4 days to lag
219 +2 day with 2 days interval.

220 As mentioned earlier, initially, at -10 and -8 days, positive rainfall anomalies are found over
221 EIO and gradually intensify and move towards MRC (Figure S1a-b). A similar propagation is
222 observed in OLR anomalies (which is regarded as a proxy for convection). At lag -4 these
223 OLR anomalies reach MRC and in the subsequent lag days, the anomalies bifurcate into two
224 cells one moving north-northwest wards towards SEPI and the second cell move southwards
225 respectively (Figure 3b). Rossby wave response to these anomalies generates a pair of
226 cyclones on either side of the equator, centered around MRC, which is seen from low-level
227 wind vectors in Figure 3b. Circulation associated with the northern hemisphere cyclonic gyre
228 advects moisture from MRC towards SEPI. A Kelvin wave response of positive OLR induces

229 easterly anomalies at lower levels towards MRC. These easterlies are more prominently seen
230 in lag -4 to -2 days over MRC. It is noticed that the presence of anti-cyclonic circulation over
231 the South China Sea (SCS) and its movement towards central India during these lags (Figure
232 3a and 3b) generate break conditions over CEN during the evolution of peak wet phase over
233 SEPI which reaffirms the contrasting nature of the wet spells over CEN and SEPI. At lag +2
234 days and after convection moves towards the west coast. Anomalous vertical velocity
235 associated with the diabatic heating due to the presence of convection (-ve OLR anomalies)
236 also indicates the apparent changes during the convection initiation over SEPI (Figure
237 2(c),2(g) and Figure 3(e)-3(h)). Evolution of the low-level winds during these composites
238 show two major aspects: a) presence of strong Kelvin wave components on the eastern edge
239 of the convection b) cyclonic circulation over SEPI and convergence on the western edge of
240 the convection. The top-heavy vertical profiles and associated upper level (200 hPa)
241 circulation exhibits divergent patterns over SE and MRC continent during the lags 0 and +2
242 days indicating an obvious baroclinic structure of convective anomalies over SEPI. The
243 space-time evolution of key variables depicts the classical *Gill* type circulations due to the
244 presence of convective anomalies around the equatorial regions which are responsible for the
245 moistening during wet spells over SEPI. Thus, it can be inferred from the present analysis
246 that the combined effect of large-scale circulation and moisture anomalies over MRC
247 contribute for moistening and subsequent positive rainfall anomalies over SEPI. Since the
248 temporal evolution of the moisture leads to rainfall (Figure S1b), for completeness, the
249 impact of moisture advection in initiating the wet spells over SEPI is discussed in
250 supplementary material.

251 **4. Summary and discussion:**

252 The present work progresses our understanding of the initiation of monsoon wet spells over
253 the rain shadow region (SEPI) in the Indian subcontinent during the boreal summer monsoon.

The SEPI experiences active monsoon conditions (Fig. 1a2) when the Central Indian (CI) region is undergoing a break phase. Here, for the first time, we report a Gill type response in initiating the wet spells over the SEPI region through the large scale wave dynamics using a composite lead-lag analysis from the long term (35 years, 1981-2015) reanalysis data.

The present analysis shows that the space-time evolution of positive rainfall anomalies that exhibits poleward propagation in both the hemispheres, from the equatorial regions leads the rainfall over SEPI. Temporal evolution of rainfall anomalies averaged over SEPI and MRC shows the lead times are ~5-7 days. Over SEPI, during the evolution of wet spell, positive q anomalies also lead by ~5-6 days institute rainfall anomalies and premoistening of the atmosphere occurs around boundary layer heights (Figure S1b). This low-level preconditioning is significantly seen over MRC (Figure 2f). Differences seen in ω' profiles over SEPI and MRC indicate the differences in the diabatic heating and corresponding cloud vertical structures. The transition from shallow to deep convection, as evidenced by CLW profiles,over SEPI largely agrees with the preconditioning of the tropospheric column during the evolution of wet spells. Presence of strong Kelvin wave components on the eastern edge of the convection and cyclonic circulation over SEPI and convergence on the western edge of the convection depicts the classical Gill type solutions to the heating associated with convective anomalies around the equatorial regions which are responsible for the moistening during the initiation of wet spells over SEPI.

Based on the analysis, the following mechanism is put forward and it is schematically shown in Figure 4. Diagnostics from the reanalysis show prioir to the initiation of the wet spells over SEPI, positive convection from the equatorial Indian Ocean regions upon reaching the MRC emanates a pair of Rossby cells on westside of the convection centre and equatorial Kelvin waves on the eastern side respectively . The westerly components of the Rossby circulation anomalies advect moisture anomalies from MRC towards SEPI and helps in the initiation of

wet spells. And from the moist thermodynamics point of view, climatological winds acting on the anomalous moisture gradients also act in commencement precipitation anomalies over the SEPI region (Figure S2). The identified mechanism and associated lead timings in the key meterological variables, during the wet spells over SEPI, has important implications for understanding and predicting the wetspells evolution in the global and regional models. Having recognized the equatorial wave dynamics in the initiation of the wet spells over SEPI, out future work will focus on column-integrated budgets and the impact of Indian ocean SST's. Though our results add supporting evidence for the several key equatorial processes, our study also made a new finding regarding the moisture availability for convection over SEPI during wet spells.

Acknolwedgements:

The data used in this study is freely available and the authors would like to thanks all centers for providing the data. We thank India Meteorological Department (IMD), Pune for providing the daily gridded rainfall observational data. The data can be obtained freely from link http://www.imdpune.gov.in/Clim_Pred_LRF_New/Grided_Data_Download.html. TRMM satellite used in the present study can be downloaded from the http://disc.sci.gsfc.nasa.gov/TRMM. Three dimensional atmospheric variables from ECMWF reanalysis prouct (ERA5) used in this study are obtained from https://climate.copernicus.eu/climate-reanalysis.

.

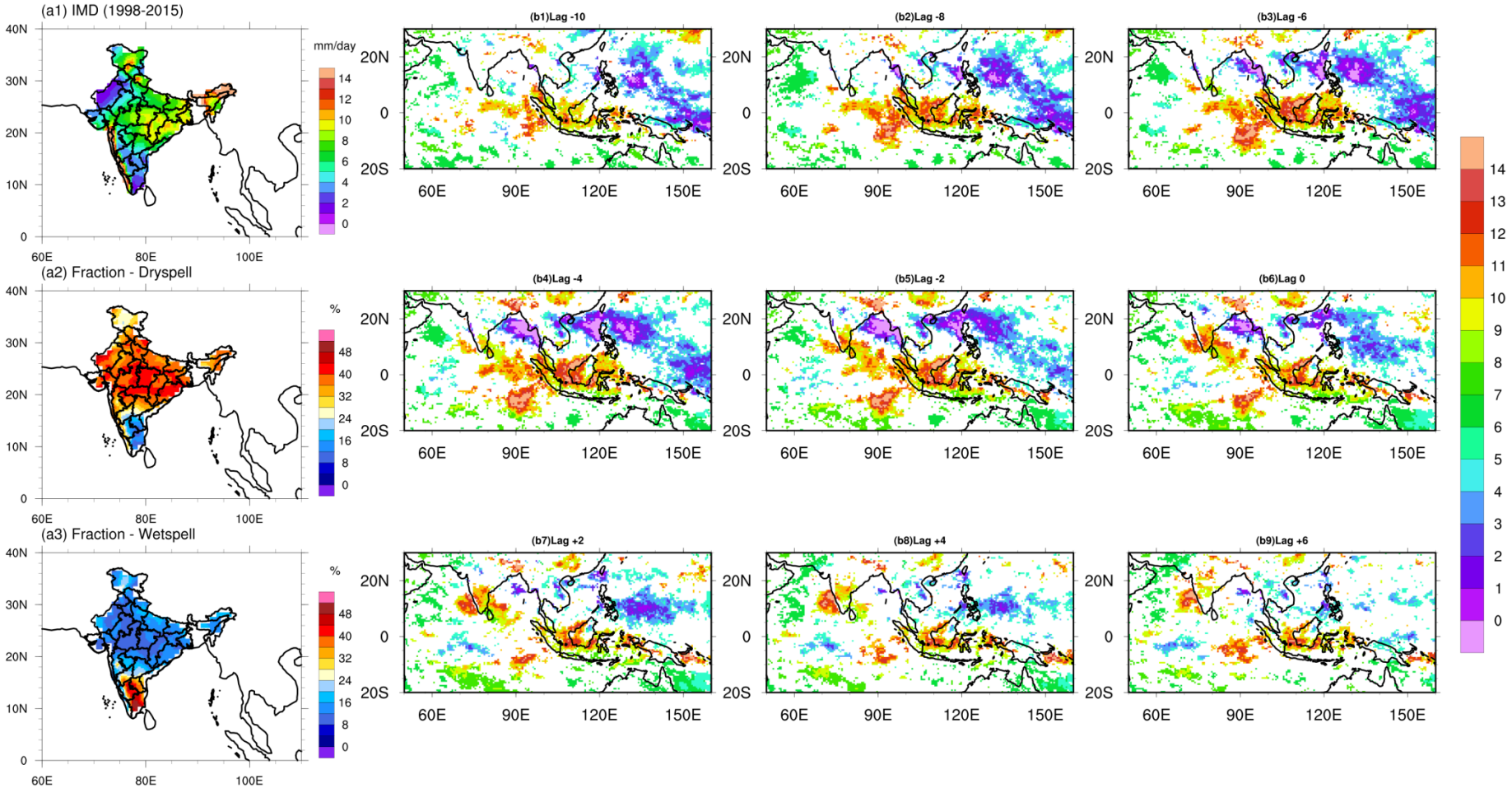

Figure 1: Spatial pattern of seasonal (June through September) rainfall (mm/day) over Indian region from (a) IMD rain gauge measurements and rainfall fraction computed during (a2) dry spell days and (a3) wet spell days over SEPI. Composite space-time evolution of rainfall anomalies from lags -10 to +6 days are shown in b1-b9. In the composite map grids with 95% confiedence levels are only shown.

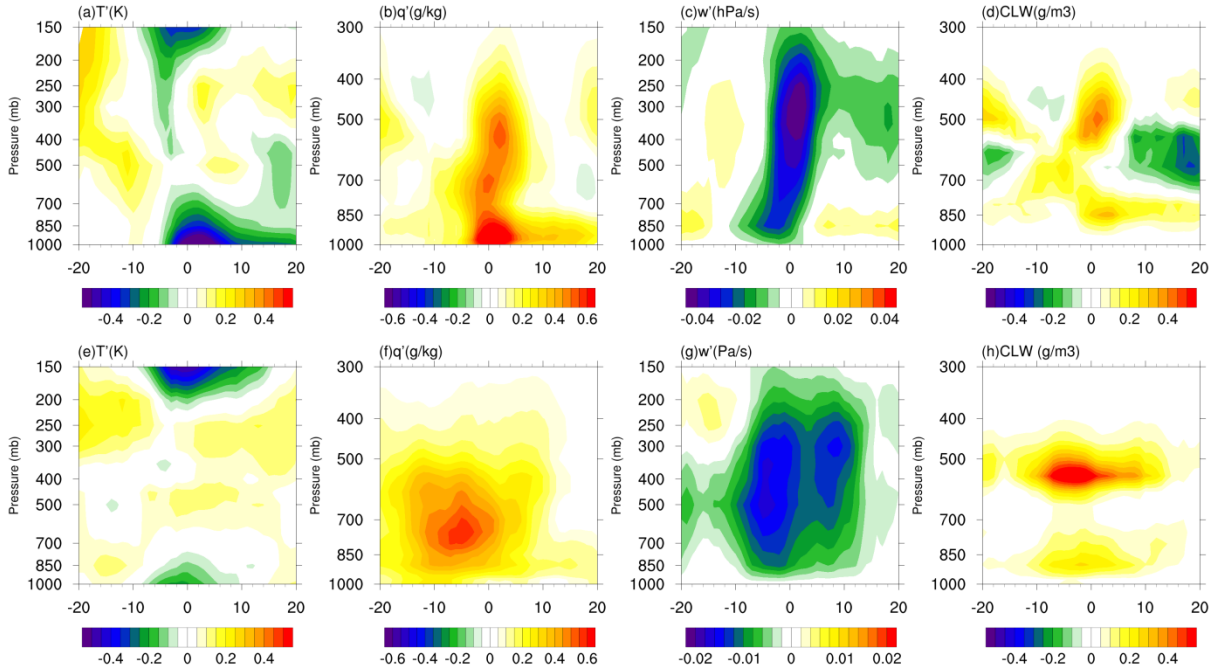

Figure 2: Composite vertical profiles of Temperature (*T*), specific humidity (*q*), vertical velocity (ω) and cloud liquid water (CLW) from ERA5 over SEPI [(a)-(d)]and MRC[(a)-(d)].

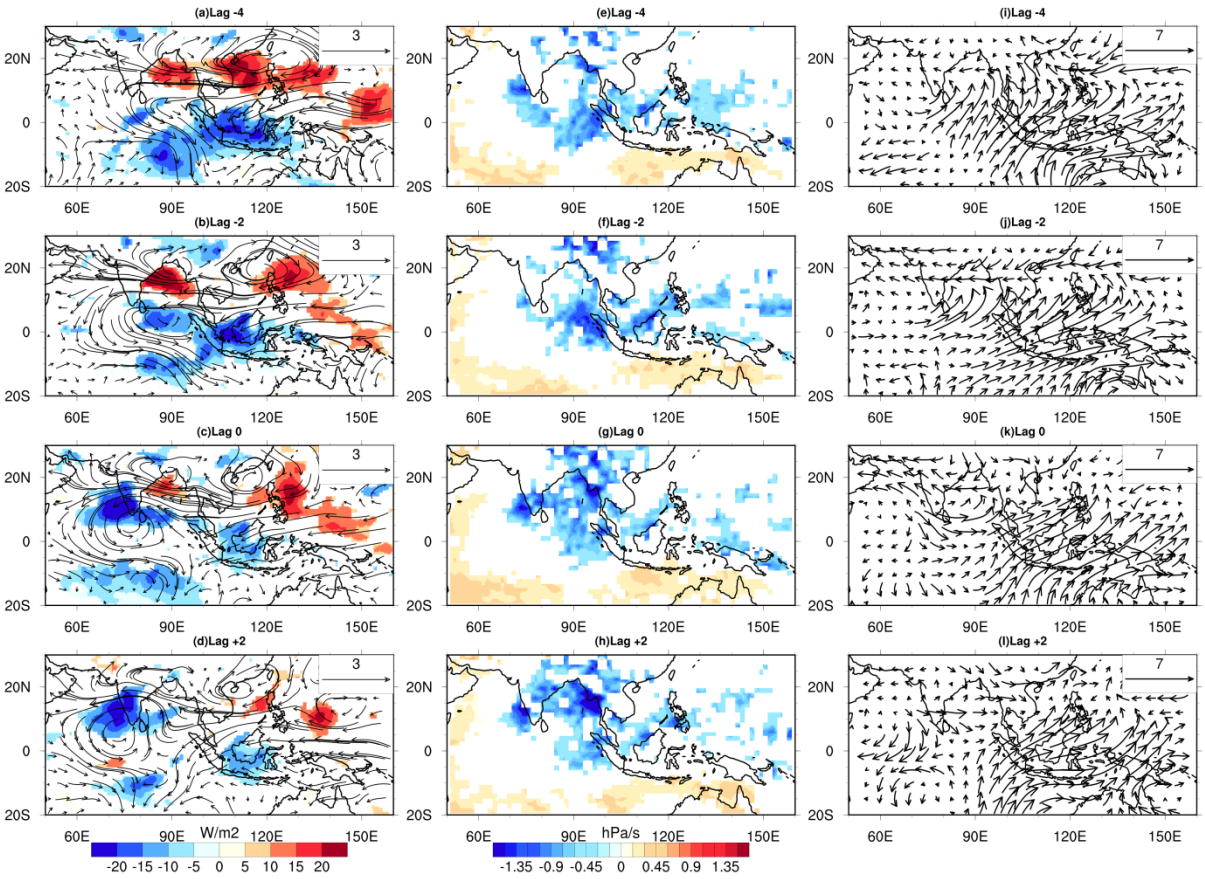

311

312

313 **Figure 3:** Spatial plots of the composite evolution of (a)-(d) OLR (Wm-2) anomalies
314 (shaded) superimposed with 850hPa wind vectors (m/s); (e)-(h) anomalous vertical velocity
315 and (i)-(l) wind anomalies at 200 hPa level. Significance of the composites is based on the
316 student's t-test. OLR anomalies with with 95% confiedence levels are only shown.
317 Composite evolutions are provided only from lag -4 to lag +2 days with 2 day intervals.

318

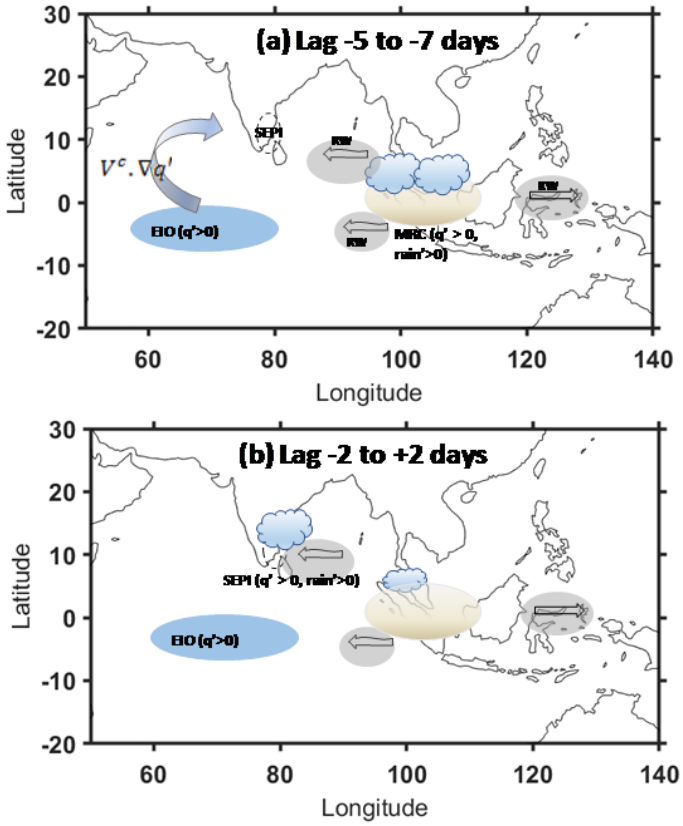

319

320 **Figure 4:**A schematic illustrating the linkage between the equatorial Indian Ocean to the
321 south east peninsular India (SEPI), during (a) lag -5 to -7 days and (b) lag -2 to +2 days
322 during boreal summer monsoon season. Blue and light yellow shaded region represents the
323 equatorial Indian Ocean (EIO) and MRC respectively. Grey ellipses on the western (eastern)
324 side show the Rossby (Kelvin) waves.

325

326

327

References:

Annamalai, H., and J. M. Slingo (2001), Active/break cycles: Diagnosis of the intraseasonal variability of the Asian Summer Monsoon. *Cli. Dyn*, **18**, 85-102.

Bhat G. S., A. Chakraborty, R. S. Nanjundiah, and J. Srinivasan (2002), Vertical thermal structure of the active and weak phases of convection over the north Bay of Bengal: Observation and model results. *Curr. Sci.* **83**, 296-302.

Chen and Wang 2018; Effects of enhanced fron walker cell on the eastward propagation of the MJO, *J. Climate*, **31**, 7719–7738

Gadgil, S. (2003), The Indian monsoon and its variability. *Annu. Rev. Earth Planet. Sci*.,**31**, 429 - 467;

Goswami , B. N (2005), The Asian monsoon Interdecadal variability, The Asian Monsoon, Eds, Bin Wang, Chapter 7, Praxis, Springer Berlin Heidelberg, 295-327pp.

Goswami, B. N., R. S. Ajaymohan, P.K. Xavier and D. Sen gupta (2003), Clustering ofsynoptic activity by Indian summer monsoon intraseasonal oscillations. *Geophys.Res. Lett.*, **30**, 1431, doi 10.1029/2002GL016734.

Goswami B. N., and R. S. Ajay Mohan (2001), Intra-seasonal oscillations and interannual variability of the Indian summer monsoon. *J. Climate.* **14**, 1180-1198;

Hersbach, H., and D. Dee, 2016: ERA5 reanalysis is in production. ECMWF Newsletter, No. 147, ECMWF, Reading, United Kingdom, https://www.ecmwf.int/en/elibrary/16299-newsletterno-147-spring-2016

Hsu, P.-C., and T. Li, (2012), Role of boundary layer moisture asymmetry in causing the eastward propagation of the Madden-Julian Oscillation, *J. Climate*, **25**, 4914–4931.

Joseph, P.V., and S. Sijikumar (2004), Intraseasonal variability of the low-level jet stream of the Asian summer monsoon, *J. Climate*, **17**, 1449–1458

Kiladis, G. N., K. H. Straub, and P. T. Haertel (2005), Zonal and vertical structure of the Madden-Julian oscillation, J. Atmos. Sci., 62, 2790 – 2809, doi:10.1175/JAS3520.1

Krishnamurti, T. N., and H. N. Bhalme (1976), Oscillations of a monsoon system. Part I.Observational aspects, *J. Atmos. Sci.* **33**, 1937–1954

Lawrence, D. M. and P. J. Webster (2002), The boreal summer intraseasonaloscillation:Relationship between northward and eastward movement of convection. *J. Atmos. Sci.*, **59**, 1593-1606

McBride J. L, and W. M Frank (1999), Relationships between stability and monsoon convection. *J. Atmos. Sci.*, **56**, 24– 36

Mohan, T.S., H. Annamalai, L. Marx, et al., 2018: Representation of ocean-atmosphere processes associated with extended monsoon episodes over South Asia in CFSv2. Frontiers Earth Sci., 10.3389/ feart.2018.00009Mohan and Rao 2012;

Mohan, T. S. and Rao, T. N., Differences in the mean wind and its diurnal variation between wet and dry spells of the monsoon over southeast India. *J. Geophys. Res*., 2016, 121(12), 6993–7006; doi:10.1002/2015JD024704;

Mohan, T.S., Rao, T.N. and Rajeevan, M. Differences in CAPE between wet and dry spells of the monsoon over the southeastern peninsular India. *Meteorol Atmos Phys* **131,** 657–668 (2019). https://doi.org/10.1007/s00703-018-0590-9

Madhulatha, A., M. Rajeevan, T. S. Mohan and S. B. Thampi 2020: Observational aspects of tropical mesoscale convective systems over southeast India. J. Earth Syst. Sci. (2020)129 65. https://doi.org/10.1007/s12040-019-1300-9

Prasanna, V., and Annamalai, H. (2012). Moist dynamics of extended monsoon breaks over south Asia. Climate J. 25, 3810–3831, doi: 10.1175/JCLI-D-11-00459.1

Rajeevan, M., J. Bhate, J. D. Kale, and B. Lal (2006), High resolution daily gridded rainfall data for the Indian region: Analysis of break and active monsoon spells. *Curr. Sci.* **91**, 296-306.

Rajeevan, M., S. Gadgil and J. Bhate (2010), Active and break spells of the Indian Summer monsoon. *J. Earth Syst. Sci.* **119**, 229–247.Webstre et al 1998.

Rao, T. N., K. N Uma, T. M. Satyanarayana, and D. N Rao (2009) Differences in draft core statistics from wet spell to dry spell over Gadanki (13.5° N, 79.2° E), India. *Mon. Weather. Rev*. **137**, 4293-4306;

Sikka, D. R. and S. Gadgil (1980), On the maximum cloud zone and the ITCZ over Indian longitude during southwest monsoon. *Mon. Wea. Rev.*, **108**, 1840–1853.

Simpson, M., Hari warrior, Sethu Raman, P. A. Aswathanarayana, U. C. Mohanty and R.Suresh (2007), Sea-breeze initiated rainfall over the east coast of India during theIndian southwest monsoon. *Nat Hazards*, **42**, 401-413

Williams, E. R., S. G. Geotis, N. Renno, S. A. Rutledge, E. Rasmussen and T. Rickenback (1992) A radar and electrical study of tropical "hot towers". *J.Atmos. Sci*., **49,** 1386-1395.

Webster, P. J., and coauthors (2002), The JASMINE Pilot study. *Bull. Am. Meteorol. Soc.* 83, 1603-1630. Hendon and Sallby 1994,

Webster, P. J., Magana, V. O., Palmer, T. N., Shukla, J., Tomas, R. A., Yanai, M. U., & Yasunari, T. (1998). Monsoons: Processes, predictability, and the prospects for prediction. *Journal of Geophysical Research: Oceans*, *103*(C7), 14451-14510.

Yasunari, T. (1979), Cloudiness fluctuation associated with the northern hemisphere summer monsoon. *J. Meteorol. Soc. Japan*, **57**, 227-242.